Mine Water Environ (2009) 28:2–14
DOI 10.1007/s10230-008-0063-3

TECHNICAL COMMUNICATION

Numerical Modeling of Geothermal Use of Mine Water: Challenges and Examples

A. Renz · Wolfram Rühaak · P. Schätzl · H.-J. G. Diersch

Received: 29 October 2008 / Accepted: 17 December 2008 / Published online: 10 January 2009

Abstract Geothermal energy, including the geothermal use of mine water, is increasingly important, due to ecological and economical reasons. Numerical flow and heat transport models can help to estimate the efficiency of such facilities. In addition, it is possible to test different configurations. However, the modeling of mine voids is challenging because it is necessary to simultaneously solve the heat transport in the surrounding porous medium and within the mine workings. Different modeling approaches are demonstrated, such as 2-D cross-sections, 2-D models with 1-D elements for the mine workings, and 3-D models. It is shown that numerical simulations can provide sufficient validity for specific modeling goals. However, none of the currently feasible modeling strategies can be seen as a perfect and fully physical solution. Suggestions are given on how to use the different approaches.

Keywords Geothermal energy · Geothermics · Heat transport · Mine water · Numerical modeling

Introduction

Geothermal energy taps the heat and cooling capacity of the solid earth and its internal fluids. It has tremendous potential, which is only starting to be tapped by mankind for space heating, process heat, and generation of electric power (e.g., Clauser 2006). One of the advantages of geothermal energy is that its use can reduce CO_2 emissions. Mine water in both operating and abandoned mines can, for example, be used for district heating systems or for pre-heating the air for mine ventilation. Recently, Watzlaf and Ackman (2006) provided an overview of the application of mine-water for geothermal usage. They indicated that annual heating and cooling costs could be reduced by 67 and 50%, respectively, for a site in Pittsburgh, Pennsylvania. The energy output–input ratio for such a system can be approximately four or higher (Wieber and Pohl 2008).

The efficient use of this natural resource can be optimized by applying numerical heat-transport models. Depending on the site, it may be necessary to take density-coupled processes into account. Furthermore, it may be crucial to consider the thermal dependence of material properties. Thus, the simultaneous modeling of heat and mass transport processes is necessary. Several simulation codes for flow and heat transport are available, featuring different numerical methods. However, the requirement to represent complex subsurface geometries for the mine workings reduces this number substantially.

Numerical modeling has been used before to estimate the efficiency of proposed geothermal mine-water applications. For instance, Malolepszy (2003) used a TOUGH2 (Pruess 1991) model to simulate heat and mass transport for geothermal energy extraction in the workings of a Polish coal mine. Raymond et al. (2008) modeled a mine in Canada, using a three dimensional (3-D) porous media (Darcy) approach, where, based on the work of Adams and Younger (2001), the flow within the mine workings was simulated by using equations for turbulent flow. For the simulation of the examples presented in this paper, FEFLOW® (Diersch 2005; Trefry and Muffels 2007) was used.

A. Renz · W. Rühaak (✉) · P. Schätzl · H.-J. G. Diersch
DHI-WASY GmbH, Waltersdorfer Str 105, 12526 Berlin, Germany
e-mail: w.ruehaak@dhi-wasy.de

Geothermics

Geothermal installations are generally distinguished between shallow (in Germany defined as boreholes with depths up to 400 m) and deep geothermics. The latter is sometimes defined by its direct usability, i.e., that it is not necessary to use heat pumps. Deep geothermal installations are primarily used for hydrothermal heating systems and for electric power generation. Mainly due to radiogenic heat production, the earth's crust generates a continental average conductive heat flow of 65 mW m^{-2} (Beardsmore and Cull 2001). Based on Fourier's law, the rate of heat flow q (W m^{-2}) between two points is given by (e.g., Carslaw and Jaeger 1959):

$$q = -\lambda \times \frac{\Delta T}{\Delta z} \quad (1)$$

Assuming an average thermal conductivity of $\lambda = 2.16$ W m^{-1} K^{-1}, temperature increases with depth at a rate of 0.03 K m^{-1}. To operate a geothermal power plant, it is necessary to at least reach the steam temperature of the working fluid. The required temperature of 100°C for water is therefore available at a depth of 3 km, assuming an average ground temperature of 10°C. However, due to advective processes, even higher temperatures might be achieved in lower depths.

The second critical issue for open geothermal systems is the required flow rate. If heat pumps are used, the necessary flow rate depends on the utilization. In case of power generation using an enhanced geothermal system, it should be at least 180 m^3 h^{-1} (Clauser 2006). To achieve this, the flow rate can be increased by hydraulic fracturing/stimulating. Figure 1 is a prototypical model for a geothermal installation using a classic doublet of boreholes. In such a case, a typical question during project planning is the forecasted lifetime of the system, before the area of influence is cooled down to the minimum working temperature.

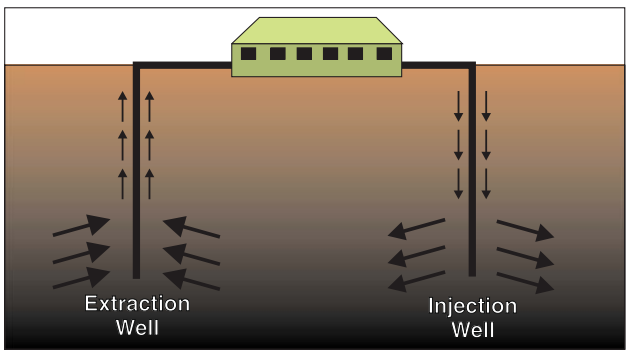

Fig. 1 Schematic illustration depicting the principle of a geothermal well installation

Based on numerical simulations, the potential cooling of the system can be assessed.

Shallow geothermics is mostly used via heat pumps together with borehole heat exchangers, taking advantage of the temperature difference between the atmosphere and the ground. Different technical solutions are used for borehole heat exchangers, e.g., u-shaped heat pipe, double u-shaped heat pipe, coaxial heat pipes, and grounding stakes. The boreholes can be filled with grout. Such ground heat exchangers, in most cases, form a vertical borehole system, where a heat carrier fluid circulates in closed pipes exchanging heat with the surrounding aquifer, driven only by thermal conductivity (a closed loop system).

Geothermal Use of Mine Water

The potential for the use of underground mines for geothermics was first investigated back in the 1970s. Water in the Springhill coal mines with a temperature of 18°C was used for geothermal energy production in Nova Scotia, Canada. Other sites include: Park Hills, USA; Follda, Norway; Shettleston, UK; and Ochil View, UK (Wolkersdorfer 2008). Recently, the geothermal energy of an abandoned coal mine in Heerlen, Netherlands, has been used (Bazargan Sabet et al. 2008).

Currently, only a small number of locations exist where mine water is being used for geothermal energy (e.g., Raymond et al. 2008). However, since the use of mine water can be profitable (e.g., Watzlaf and Ackman 2006), a large number of studies have been carried out to assess potentially suitable sites (e.g., Clauser et al. 2005; Van Tongeren and Dreesen 2004; Wieber and Pohl 2008; Wolkersdorfer 2008). Coal mines are considered promising candidates for exploiting geothermal energy (Watzlaf and Ackman 2006). The most cost-effective way is to use the heat of water already being pumped for dewatering or treatment purposes. However, mine sites may have a long history, which introduces additional difficulties to accurate numerical modeling. Another complexity associated with understanding the thermal and hydraulic system is the lateral and vertical interconnectivity of different parts of a mine, for example in multiple-seam coal mining (Watzlaf and Ackman 2006).

Depending on the available temperature, mine water can either be directly used for heating purposes or heat pumps can be used. Both closed loop and open loop systems are used; in the latter, water is abstracted, cooled down in a heat exchanger and injected at a different location (Watzlaf and Ackman 2006). In combined heating/cooling systems, abstraction and injection boreholes are often switched seasonally to take advantage of the heat storage capacity of the mine.

Numerical Modeling of Heat Transport in Mine Workings

In previous studies, a number of different approaches have been used to simulate fluid flow within mine workings (e.g., Rapantova et al. 2007). No standard approach has emerged yet, though the strong influence of pre-existing simulation codes on the simulation strategies can be noted. Representations of mining voids in the literature range from 3-D Navier–Stokes calculations (cited in Wolkersdorfer 2008) through different 3-D porous media approaches combined with 1-D pipe flow (Adams and Parkin 2002; Reymond and Therrien 2008) and hybrid finite element mixing cell approaches (Brouyère et al. 2008) to Darcy flow for both host rock and mine workings (Malolepsy 2003). To choose an appropriate simulation strategy for mine voids, it is important to decide on the flow equation and on the required dimension (1-D, 2-D, or 3-D) based on the physical properties of the system to model.

Flow Equation

While a 3-D simulation using the Navier–Stokes equations would be the most accurate approach, covering situations of both laminar and turbulent flows, this seems unfeasible for entire mine systems due to the high numerical demand (Wolkersdorfer 2008). Most empirical flow equations, however, are only applicable for flow within a certain range of the Reynolds number (e.g., White and White 2005). Due to the high roughness and large diameter of the mine voids, flow can be assumed as nearly always turbulent (Wolkersdorfer 2008), while in backfilled parts or goaf material, laminar flow is expected. Equations for laminar fluid flow, such as Darcy's equation (e.g., Diersch 2005) and the equation of Hagen and Poiseuille (e.g., Diersch 2005), assume a linear dependency of flow velocity on the gradient of hydraulic head. Under turbulent flow conditions, this assumption is no longer valid. Empirical flow equations for turbulent flow, such as Manning's equation (e.g., Diersch 2005), can provide a better approximation here. Figure 2 shows a schematic comparison of flow velocities obtained for a mine shaft using different equations (roughness/hydraulic conductivity parameters not fully equivalent).

Dimension

The voids of an abandoned mine in many cases are not extended widely in all three dimensions. In comparison with the surrounding rock mass, shafts or tunnels may be considered as one-dimensional, while mined coal seams can be approximated as two-dimensional. Such geometrical simplifications allow easier application of empirical flow equations for turbulent fluid flow, such as Manning's equation. Reducing the mine workings to one-dimensional structures, combined 1-D/3-D simulation models, such as SHETRAN-VSS (Adams and Parkin 2002), and combined 1-D/2-D/3-D models such as FEFLOW (Diersch 2005) or HydroGeoSphere (Raymond and Therrien 2007) can be applied.

However, the reduction of flow geometry may not be suitable in all cases. At higher Rayleigh numbers, the development of convection cells is possible, supporting heat transport in the system. In contrast to larger

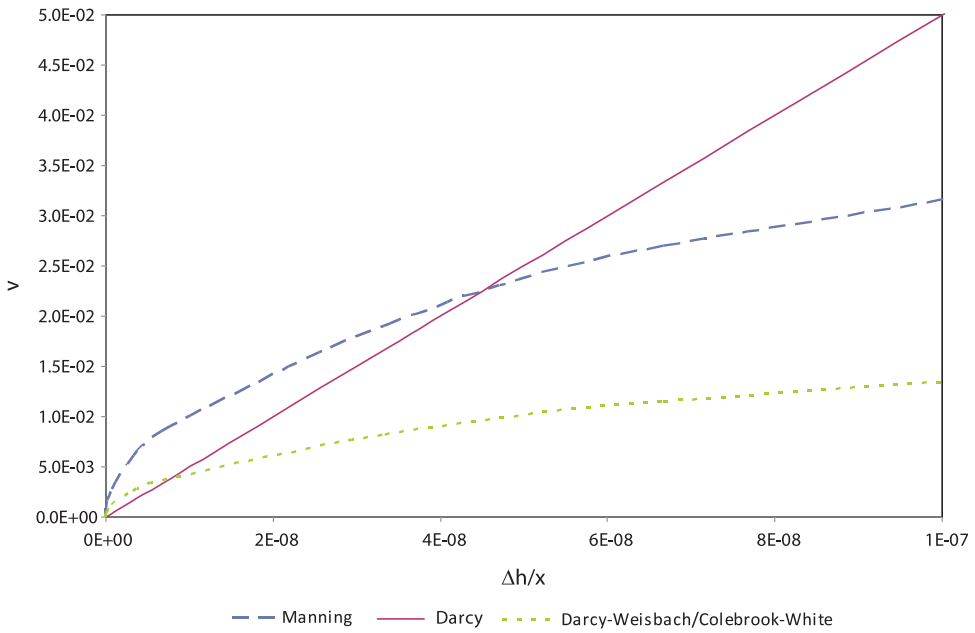

Fig. 2 Schematic comparison flow velocities calculated by the equations of Manning, Darcy, and Darcy–Weisbach for different differentials of hydraulic head at a mine shaft

convection cells incorporating different shafts and tunnels, these local convection cells cannot be simulated in 1-D or 2-D approximations of the workings. The imprecise geometrical implementation could significantly influence the heat transport behavior of the system. The empirical equations for turbulent flow relate to 1-D pipe or channel flow and are not directly applicable to a 3-D implementation. Thus, in the example calculations further below, Darcy's law has been applied for all 2-D and 3-D calculations of mine workings. However, it has to be kept in mind that a linear scaling of velocity with head difference is not realistic. Therefore, the hydraulic conductivity parameter in such applications should be adapted according to the expected Reynolds number.

Temperature Dependence

Density variation due to changes of the temperature is taken into account by applying a sixth order polynomial (Diersch 2005):

$$\rho(T) = a + b \times T + c \times T^2 + d \times T^3 + e \times T^4 + f \times T^5 + g \times T^6 \quad (2)$$

By using values of $a = 10^3$, $b = 6.76 \times 10^{-2}$, $c = -8.99 \times 10^{-3}$, $d = 9.14 \times 10^{-5}$, $e = -8.91 \times 10^{-7}$, $f = 5.29 \times 10^{-9}$, $g = -1.36 \times 10^{-11}$, a relationship (Fig. 3) results. Pressure dependence is neglected here because the depth of the following modeling examples is below 800 m. Density dependence due to salinity is neglected, too. However, the software is able to take density variations due to heat and mass-transfer simultaneously into account.

Temperature dependence is introduced by the scalar hydraulic conductivity, K (m s^{-2}):

$$K = k\rho_f g/\mu_f \quad (3)$$

with: μ_f (Pa s) denoting dynamic fluid viscosity, ρ_f (kg m^{-3}) fluid density, k (m^2) permeability, and g (m s^{-2}) gravity. Due to the temperature dependence of the dynamic viscosity, the hydraulic conductivity decreases approximately 2/3 at 26°C compared to the value at 10°C. However, this dependence is neglected in the following numerical calculations. The main reason for this is that the lower-dimensional elements that are used in the code do not take viscosity changes into account.

Limitations of the Numerical Precision

The very strong parameter contrast between the highly conductive mine workings and the much less conductive host rock introduces numerical challenges to the computation. Notwithstanding the weak performance of mathematical emulators, the precision of every floating point operation in a numerical model is limited to a certain number of digits (the numerical precision), which is based on the CPUs architecture (e.g., Goldberg 1991). If the difference of two numbers is orders of magnitude smaller than the actual numerical precision, the resulting matrix cannot be calculated correctly; a random result may be the consequence due to deletion of the last digits.

In this model, the difference of piezometric head values between two highly conductive elements is typically a very small number; in the applications shown below, it is around 10^{-13} m. If the total head value exceeds 10^{-3} m, these

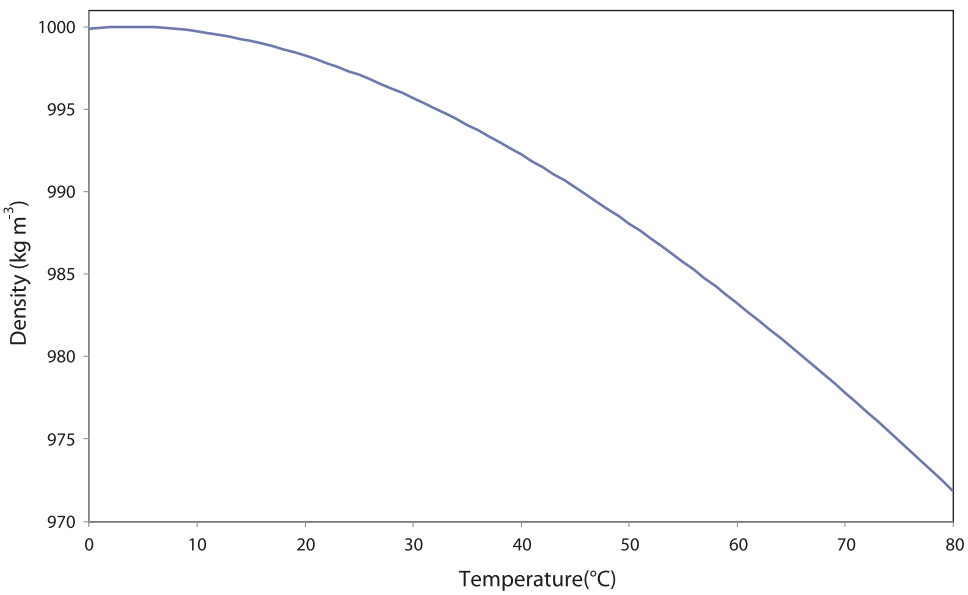

Fig. 3 Graph showing the used temperature dependent water density

differences may not be calculated correctly on an Intel x86- or x64-based CPU, where approximately 10–12 significant digits are available in double precision. Therefore, in this study, a fixed potential of $h = 0$ m has been assigned at the extraction point within the mine voids to minimize the occurrence of absolute hydraulic head values in the model. All numerical simulations have been computed on a dated DEC Alpha system, which features a higher numerical precision of 80 bits. In the future, this shortcoming can be circumvented by using the more precise 'long double' data type in the code.

A Type Study

For this conceptual study, we used data that was available for an abandoned salt-mine, even though salt mines can probably not be used for open-loop geothermal energy production due to the risk of collapsing mine voids caused by salt dissolution. As already stated, abandoned coal mines are much more promising sites but we did not have access to data from such mines. We intentionally did not consider the effects of density due to the salinity of the water; the fact that a salt-mine was used is therefore reflected only in the geometry of the mine workings. We believe that for the type of conceptual model being discussed here, the differences in the mine structure could be temporarily ignored. However, it is important to point out that the project is at an early stage, so the data validity is still weak.

2-D Model

A 2-D model was set up to compare different approaches for modeling the geothermal use of mining structures. It is common practice to represent mining voids as porous media with a very large hydraulic conductivity (K), which is ideally fitted to measured data (see e.g., Clauser et al. 2005). Results obtained by applying lower-dimensional finite elements can be applied by using different flow equations: Darcy, Hagen–Poiseuille (laminar pipe flow), and Manning–Strickler (turbulent flow). In addition, the influence of density effects not related to salinity was analyzed.

Model Description

The model geometry was based on an abandoned potassium mine in Staßfurt, Germany. The mine was developed during the 19th century and was one of the first subsurface potassium mines in the world. It was closed down in the 1920s and is completely flooded. The 2-D model is based on a geological cross section through the central part of the salt dome (Fig. 4). The different geological units and their properties are shown in Table 1.

Due to their history, the structure of these mine workings is highly irregular, compared to today's mines. In the following discussion, the elements of the mine workings are classified into four types: shafts, roadways, drivings, and caverns.

Two primary shafts were developed for mine access; these provide the major avenues for vertical fluid flow and are the only remaining accessible openings of the mine. In addition, several secondary shafts interconnect the drivings on different horizons. For simplicity, we assumed the same geometry for all shafts: vertical, open (not filled), and having a square cross-sectional area of 20 m^2. The shaft sealing was assumed to be concrete.

Roadways connect different parts of the mine in the horizontal direction. For simplicity, all roadways were considered as tunnels with a square 25 m^2cross section,

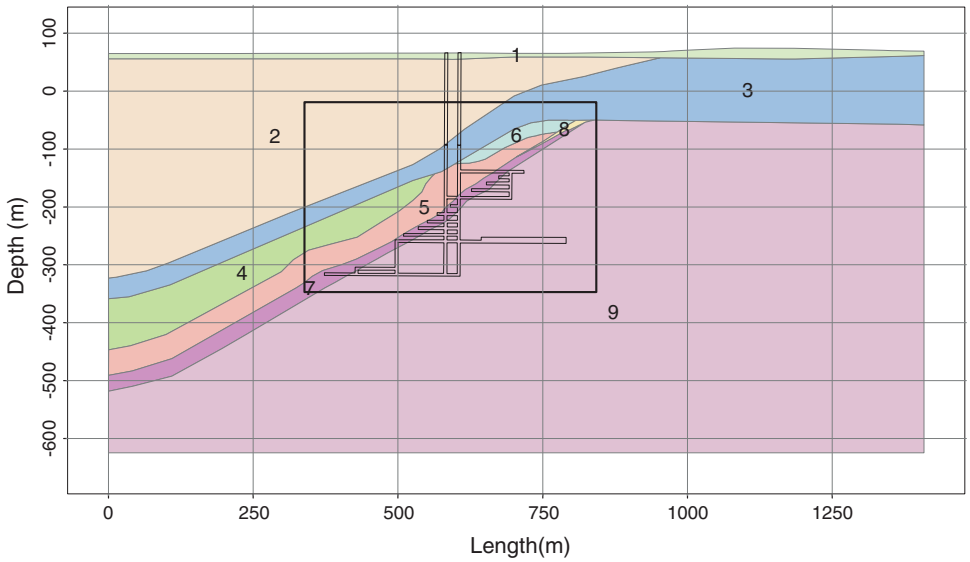

Fig. 4 Geologic structure of the 2-D model (numbered geological units are explained in Table 1) and mine workings. The *black rectangle* marks the area shown in the result figures

Table 1 Geological units and associated physical properties

ID	Rock type	Porosity n (−)	Hydraulic conductivity K (m s^{-1})	Volumetric heat capacity ρc (10^6 J m^{-3}3 K^{-1})	Heat conductivity λ (W m^{-1} K^{-1})
1	Quaternary	0.2	5×10^{-5}	2	1.8
2	Lower Triassic	0.08	1×10^{-7}	2	2.2
3	Cap rock	0.05	5×10^{-6}	2	2.0
4	Halite	0.01	1×10^{-10}	1	5.0
5	Anhydrite	0.05	5×10^{-6}	2	2.5
6	Dissolved anhydrite	0.1	1×10^{-5}	2	2.0
7	Sylvite	0.01	1×10^{-8}	1	5.0
8	Dissolved sylvite	0.1	1×10^{-5}	1	4.0
9	Halite	0.01	1×10^{-10}	1	5.0

Table 2 Laws and parameters for flow and transport calculation in 1-D finite elements

Type of mine structure	Cross section (m^2)	Roughness coefficient ($m^{1/3}$ s^{-1})	r_{hydr} (m)	K (grad h)$^{1/2}$ (m s^{-1})	Length-specific heat storage (J K^{-1} m^{-1})
Elements of turbulent flow regime: calculation with Manning–Strickler law for submerged quadratic tube					
Open shaft	19.81	81.4	1.11	8.74×10^1	8.32×10^7
Roadway	25.00	40.0	1.25	4.64×10^1	1.05×10^8
Elements of laminar flow regime: calculation with Hagen–Poiseuille law					
Driving	1,500.00	5.0	2.50	5.66×10^9	6.30×10^9
Cavern	3,000.00	10.0	5.00	2.26×10^{10}	1.26×10^{10}

assuming that the walls were roughly excavated and that the bottom was paved.

The stopes were assumed to be filled with water at a temperature in equilibrium with the surrounding rock mass. Extraction and injection wells were simulated; at the latter, the temperature is lower than the extraction temperature.

The movement of water within the subsurface was calculated using Darcy's equation. The flow in the mining structures (shafts, roadways, drivings, caverns, see Fig. 5) is free fluid movement. Volumes where turbulent flow is expected were calculated using the Manning–Strickler equation; for slow-moving laminar flow, the Hagen–Poiseuille equation was applied. The respective equations and parameters used for the different types of mine structures are summarized in Table 2.

Roadways and shafts are the primary flow paths, with relatively high velocities. Considering the typical high roughness of mining galleries, turbulent flow is likely within these structures. We expect the major pressure loss of the system here.

In contrast, the velocities in drivings and caverns are expected to be very small, leading to the assumption of a laminar flow regime. These structures represent the largest voids in the mine. They cover the major part of the mine horizon and therefore contain the major portion of the mine water.

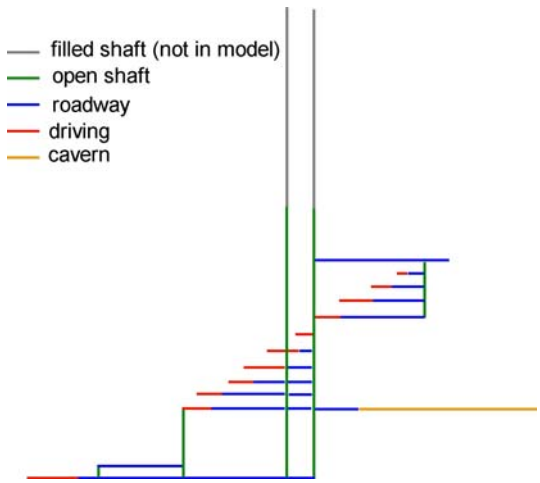

Fig. 5 Types of mine structures in the model

Drivings and caverns were considered to have roof elevations of 5 and 10 m, respectively. However, the main part of their extent (several hundred meters) is orthogonal to the projected 2-D model area. This model therefore restricts the possibility of incorporating the real behavior of flow and transport in these voids. To represent their ability to store large amounts of water and therefore thermal energy, a heat capacity equivalent to the complete depth was applied to the 1-D elements representing the void.

The numerical model is based on the finite-element simulator FEFLOW, which features capabilities to include both porous media (Darcy) type flow calculations and lower-dimensional discrete elements for laminar or turbulent flow in a density-coupled simulation.

The cross section of the salt dome was discretized by a 2-D triangular mesh with a resolution that ranged from 3 m close to the mine to 14 m at the lower boundary (45,000 elements in total). These elements were used for the Darcy flow calculation. For the calculation of the laminar and turbulent flow in the mining structures, additional 1-D elements were applied. For simplification, all outer model boundaries were considered to be impermeable for water. A hydraulic head, $h = 0$ m, was imposed at the position of the later extraction point in the upper part of the mine (see Fig. 6).

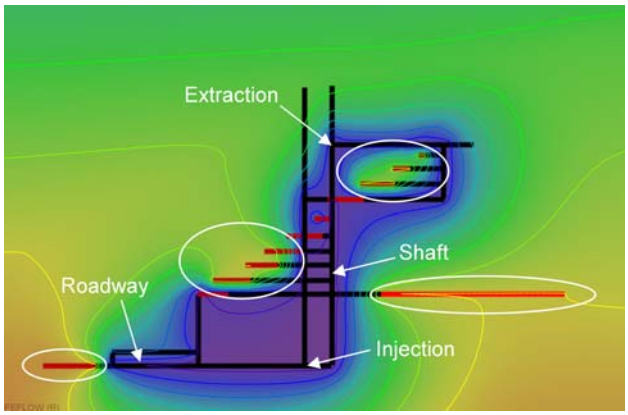

Fig. 6 Temperature distribution after 20 years of operation (position according to Fig. 4). Drivings and caverns (*red lines*) act as major heat storages. Heat dissipation is delayed here (*white circles*)

While keeping a fixed temperature of 10°C at the surface (top boundary), a constant geothermal heat flux of 65 mW m^{-2} was defined for the bottom boundary. Initial conditions were calculated from the boundary conditions in a steady-state simulation without injection and extraction of mine water. The simulation was performed for both a density-coupled model and a non-density coupled model to obtain information about the effect of temperature-dependent density in the modelled system.

There is very little difference in the temperature distribution in the results of the density-dependent and non-dependent cases. Movement due to free convection in the density-dependent simulation was negligible. As shown in Fig. 7, the velocities were all below 1 mm day^{-1}. Obviously, the temperature difference of 3.2 K within the cavern together with the geometry does not lead to a significant convective circulation system. However, this result is based on a simplified 2-D model; real world data are generally different, of course. The respective result of the non-density coupled simulation is not shown since there was no fluid movement.

In modelling the operation of a geothermal heating facility, the cold water was injected at the bottom of the shaft at a constant temperature of 3°C and a flow rate of 120 m^3 day^{-1}. This corresponds to one complete exchange

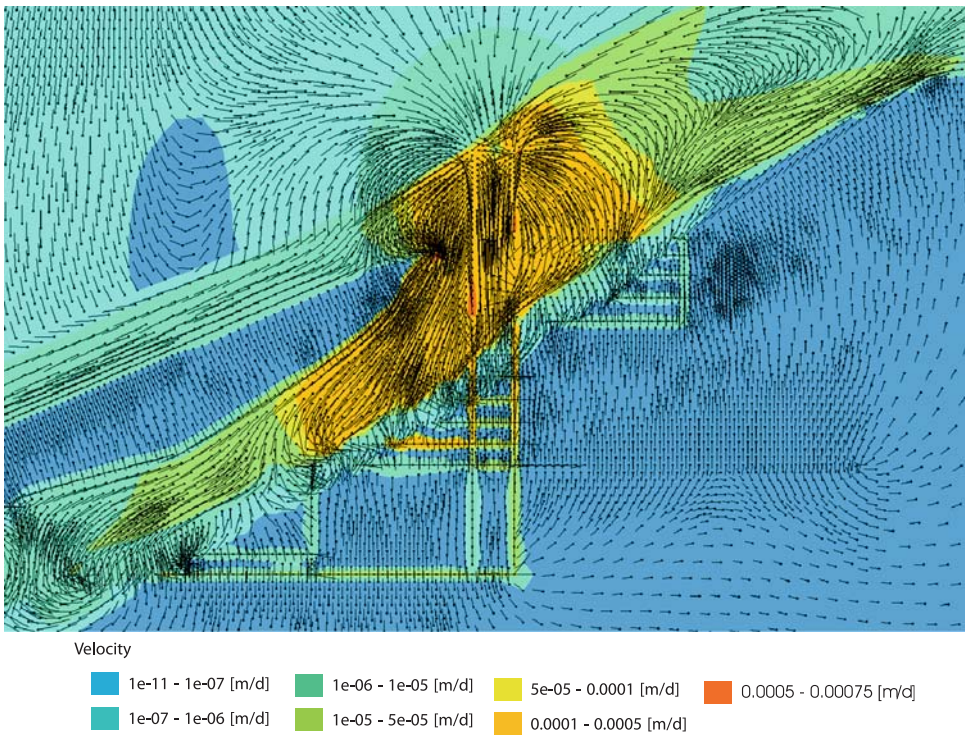

Fig. 7 Velocity distribution in the density-dependent model (position according to Fig. 4)

of the free mine water within the total simulation time of 20 years. The water can only leave the system through the extraction point in the upper part of the shaft. This dimensionless approach was used to ease comparison to models with different total mine volume.

Result of 1-D Elements

For a comparison between density-dependent and non-dependent results, the focus is on the temporal development of the extraction temperature, which is the most critical measure for the geothermal use of the water. Comparing the temperature curves shows that the density effects were insignificant (Fig. 8).

A very steep drop of the extraction temperature is observed in Fig. 8, showing that a short circuit between injection and extraction well occurs at a very early stage. Only the water in the shafts and tunnels is circulating; the caverns and drivings are almost unaffected by the pumping. The water is flowing along the shortest way between injection and extraction well, leaving the big reservoirs unused. It is obvious that the effective usage of the mine as a geothermal heat source can be improved by measures like artificial flow barriers to redirect the flow through the drivings.

The Manning–Strickler equation, which usually describes flow in channels or pipes, contains a roughness coefficient as a parameter that determines the pressure loss due to friction between the fluid and the channel wall. A major challenge in the modelling of flooded mines is to determine this parameter, since the galleries are usually inaccessible. Since these parameters always carry a high vagueness, a sensitivity study was performed to assess the impact of this uncertainty on the modelling result. The Strickler coefficient was gradually varied over a range that covered all of the types of mine walls that can reasonably be expected. As an upper limit, a value of 80 $m^{1/3}$ s^{-1} was chosen, representing a concrete wall. The lower limit of 20 $m^{1/3}$ s^{-1} corresponds to a very rough excavation.

Figure 9 shows that the chosen Strickler coefficients have little influence on the modelled temperature development. This can easily be explained by comparing the flow velocities within the shaft (approx. 3.7 m day^{-1} below the extraction point) and in the surrounding rock (far below 10^{-10} m day^{-1} at a distance of several meters next to the shaft). The total flux is fixed due to the pumping rate, so a difference in the hydraulic conductivity of the elements can only change the ratio between flux in the voids and flux in the porous medium. Since the flux in the porous medium is lower by many orders of magnitude, it is not significant for any Strickler coefficient that can reasonably be chosen for mine modelling.

Comparison with the Porous Media Approach

The classical approach to model the flow in excavations in a Darcy flow model is to treat the void as a porous medium with a very high conductivity. For the purpose of comparing both techniques, a second 2-D model was set up using this alternative approach.

The hydraulic conductivity values of the elements do not have a physical real-world representation. The impact of this new uncertainty is assessed in another sensitivity study, with values ranging from $K = 5 \times 10^{-4}$ m s^{-1} to 50 m s^{-1} (equivalent to a parameter contrast between host rock and porous medium of 10^2–10^7). The resulting temperature curves are shown in Fig. 10.

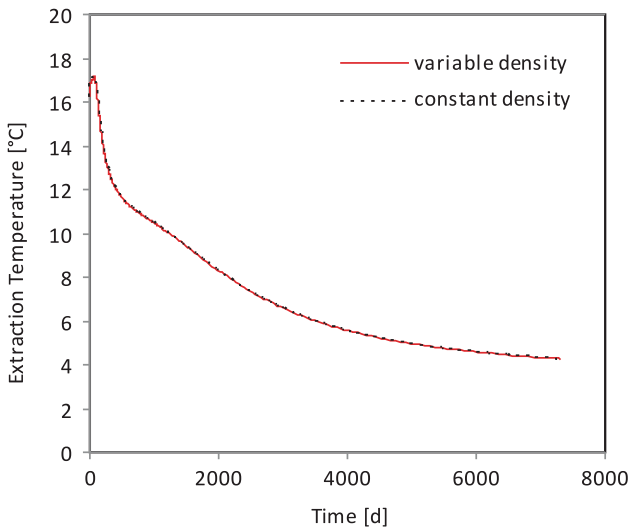

Fig. 8 Comparison of the extraction temperatures of the density-dependent and non-density dependent models

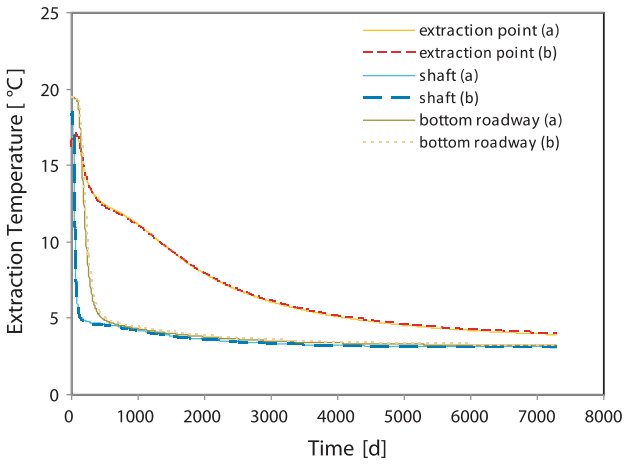

Fig. 9 Temperature development in the shaft at different observation points (see Fig. 6): **a** simulation results using $k_{st} = 20$ $m^{1/3}$ s^{-1}, **b** simulation results using $k_{st} = 80$ $m^{1/3}$ s^{-1}

As in the combined 1-D/2-D model, the temperature decreases after the cold water from the injection well reaches the extraction well. For low conductivities (contrasts of 10^2, 10^3, and 10^4 between rock and void), the decrease of the extraction temperature becomes less steep at the higher conductivities (Fig. 11). This trend vanishes after the contrast exceeds 10^5 m s^{-1} and gains significance with higher hydraulic conductivity values. At the highest parameter contrast in the study (10^7), the temperature drops immediately after the start of the simulation (after less than 3 years) below 7°C.

When using low hydraulic conductivity values for the voids, the cold water migrates into the galleries of the lowest horizon first due to the density dependency. This becomes more pronounced at higher roadway hydraulic conductivities. The cold water in the lower parts of the mine remains separated from the warm water in the upper parts.

Up to a certain optimum, near $K = 10^4$ m s^{-1}, this effect is dominant. For conductivities above this value, stronger mixing of warm and cold water can be observed, which leads to faster transport of cold water to the extraction well. The reason for this effect is the incipient effect of free convection that becomes established within the mine voids. Convection cells appear, which leads to additional mixing of water in the vertical (in the shafts) as well as in the horizontal direction (in the roadways and voids). These convection cells also cause the fluctuation of the temperature curve for $K = 50$ m s^{-1} in Fig. 10. Figure 12 exemplifies the occurrence of this effect within the cavern structure (compare to Fig. 5).

At this point, the major benefit of the porous medium approach becomes visible, as free convection effects are taken into account. However, the overall heat storage depletes fast, for the large voids of the drivings and caverns cannot be properly accounted for. Because the combined 1-D/2-D model does not have this shortcoming, it seems feasible to combine both approaches in later work to incorporate the advantages of both.

The study also shows the complex dynamic behavior of the free fluid flow during pumping. It can be seen that a stable layering of cold water under warm water is possible only for a certain range of hydraulic conductivity values (where the hydraulic conductivity is high enough to allow density-driven fluid movement without admitting the establishment of free convection).

Besides creating flow barriers in the mine, re-injecting water into stopes with poorer connectivity to the main roadways and shafts appears to be a possible measure to influence the effective usability of the system. For other,

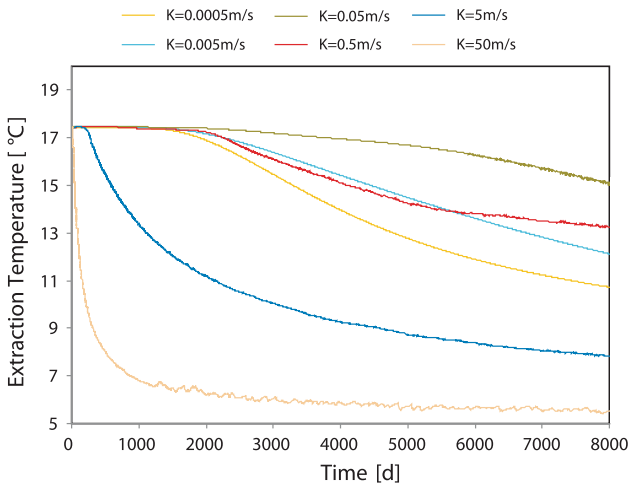

Fig. 10 Extraction temperature results of models with different conductivities K of the mine voids

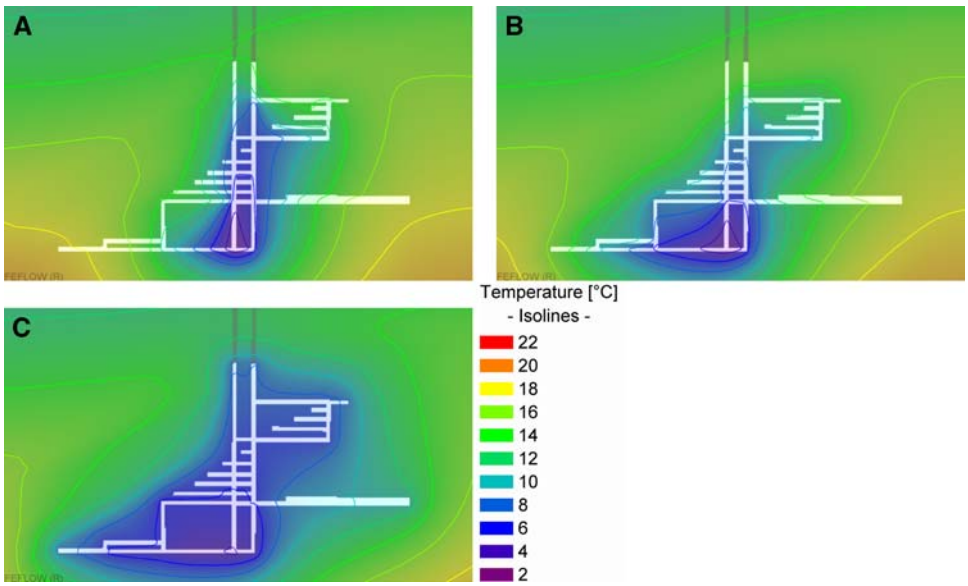

Fig. 11 Temperature distribution after 20 years with hydraulic conductivities of:
a 5×10^2 m s^{-1},
b 5×10^4 m s^{-1}, and
c 5×10^6 m s^{-1}, respectively

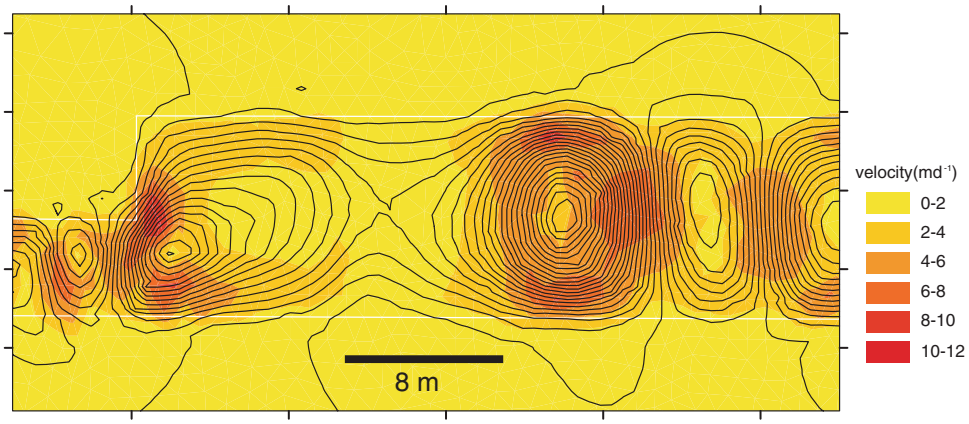

Fig. 12 Streamlines and velocity distribution in the mining voids, the data are from a model with $K = 5 \times 10^6$ m s^{-1}

potentially more complex cases, numerical modelling in 3-D will be essential.

3-D Model

As discussed before, 2-D models can be helpful for testing different geothermal set-ups and to study the influence of parameter variations. However, they are not able to give volumetric information, which is necessary since the mine workings are three dimensional. For instance, it is necessary to compute a 3-D model to get information on the heat transfer resulting from the operation. A simple approach for such a model is shown below.

Description

Although the 3-D model is a direct extension of the 2-D model discussed before, there are some differences. With respect to the units listed in Table 1, only units 1, 2, 4, 7 and 9 were assigned. In addition, a new unit was included, which represents Tertiary rocks, which are missing at the location of the cross-section discussed before. The associated parameters are: $n = 0.2$ (−), $K = 1 \times 10^{-7}$ (m s^{-1}), $\rho c = 2 \times 10^6$ (J m^{-3}3 K^{-1}), $\lambda = 2$ (W m^{-1} K^{-1}).

The volume of the water-filled mine workings is approximately 2.18×10^6 m^3. In accordance with the 2-D model, the pumping rate was set to 300 m^3 day^{-1}, enabling a theoretical complete exchange of the mine water during a pumping time of 20 years.

The dimension of the model is 5 km in the x-direction and 5 km in the y-direction (see Fig. 13). The depth extent is from −750 m up to the variable topography (approximately 70 m above sea level). The model is density dependent, according to Eq. 2.

As discussed before, the application of discrete lower dimensional elements for this modeling approach is limited. The 3-D model was therefore implemented using a 3-D porous media approach, despite all of its shortcomings. However, the presented solution gives an idea of the possibilities of applying 3-D models for geothermal mine water applications. Furthermore, such a result may be sufficient for a lot of problems. The values applied for the shafts and caverns (including drivings and roadways) are: $n = 1$ (−), $K = 5$ (m s^{-1}), $\rho c = 4.2 \times 10^6$ (J m^{-3}3 K^{-1}), and $\lambda = 0.65$ (W m^{-1} K^{-1}), according to the respective values of water.

The caverns were realized at a depth of −260 and −310 m below sea-level, respectively; two shafts connect them with the surface (see Fig. 14). As no data about the real height of the caverns exist, they were assigned a constant height of 10 m.

The flow boundary conditions (BC) are a fixed head BC at the surface according to the main river in the area (see Fig. 13). An additional recharge of 90 mm a^{-1} was assigned on the top slice. All other boundaries were assumed to be impermeable for water flow. The thermal BC were a fixed temperature at the surface of 10°C and a heat flux BC of 65 mW m^{-2} at the bottom slice. The model has approximately 1.2 million triangular prismatic elements, with approximately 600,000 nodes, respectively.

The initial state was again obtained from a quasi steady-state result. Based on this model, the geothermal mine water usage was modeled by assigning an extraction well at the bottom of the deepest shaft and an injection well with a fixed temperature of 3°C at the bottom of the model.

Results

A general overview of the model and the calculated temperature is shown in Fig. 14. The heat transfer resulting from the geothermal operation was calculated based on the equation:

$$Q = (T_{\text{out}} - T_{\text{in}}) \times (\rho c)_{\text{f}} \times q \quad (4)$$

Here Q is the amount of heat transferred (W), T_{out} and T_{in} are the temperatures at the extraction and injection well,

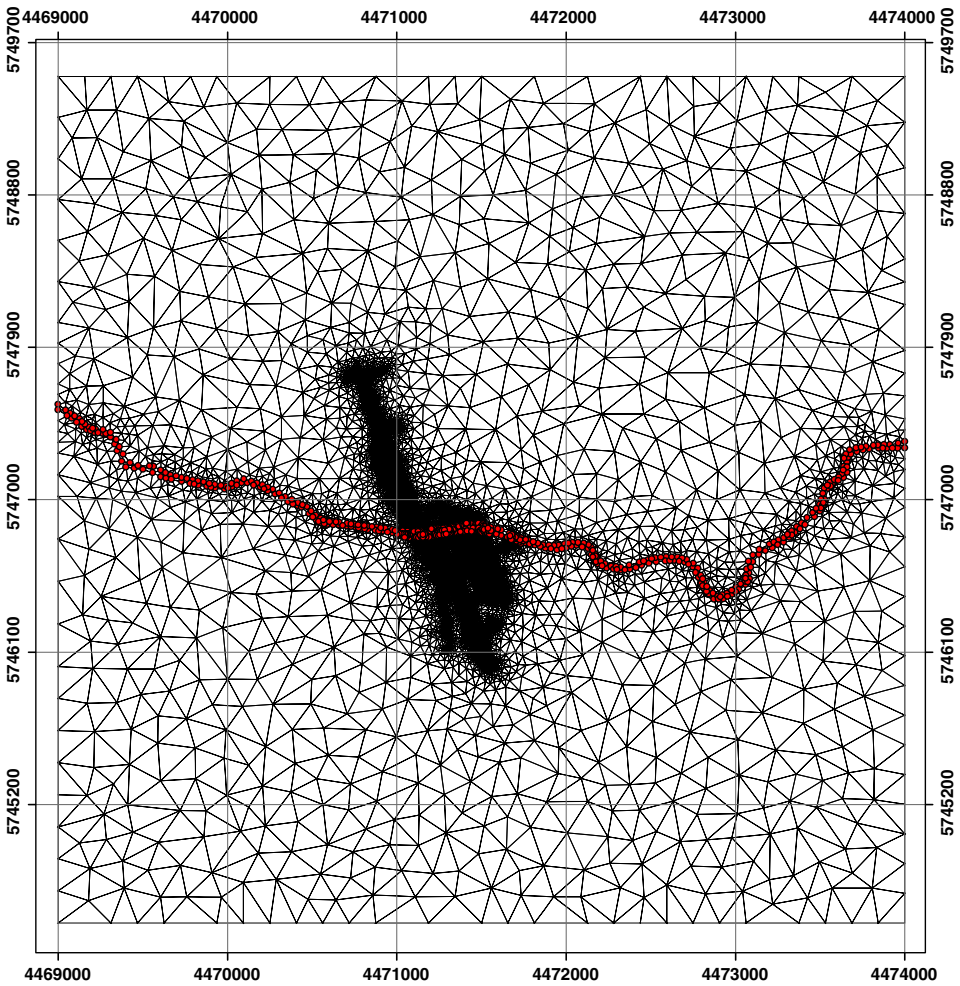

Fig. 13 Model mesh and head boundary condition, according to the main river in the area; horizontal coordinates are given in the Gauß-Krüger system

respectively (°C), $(\rho c)_f$ is the volumetric heat capacity of the fluid (4.2×10^6 J m^{-3} K^{-1}), and q (300 m^3 day^{-1}) is the flow rate. The resulting temporal heat transfer is shown in Fig. 15. The arithmetic mean is approximately 100,000 W.

Similar to the 2-D model, the temperature decreases very fast at the extraction well. Obviously, the measures to prevent a thermal short circuit are still insufficient. The temperature is constantly oscillating over time within a range of approximately −0.7 to +0.65 K at the extraction well. This oscillation is a result of free convection within the caverns. Due to differences in the lateral temperature, the convection is partly horizontal.

As shown by Fig. 15, the transferred heat decreases, after a fast drawdown at the beginning, very slowly for the given time period of 20 years. However, the total amount of heat could be significantly higher if more efficient measures were taken to prevent thermal short-circuiting between the extraction and injection well. The simplest solution would be to inject the cooled water further away.

Conclusions

Different examples of the numerical modeling of geothermal mine-water usage have been given. As 2-D models have the advantage of fast model set-up and short computation times, they are appropriate for preliminary studies. For example, they can be used for sensitivity studies and to test different numerical approaches, such as porous media compared to lower dimensional discrete elements. However, for calibration and prognostic aims, it is necessary to compute a 3-D model.

This study revealed some shortcomings of the applied modeling system. The main problem is the simultaneous (non-sequential) solution of pipe-flow together with the remaining matrix. Due to extreme parameter contrasts, together with a very small head gradient, this leads to stiff matrices that are difficult to compute and, even more problematic, to serious problems due to the limited representation of floating point numbers. In the future, this problem will be addressed by applying the more precise ‘long double’ data type in the code.

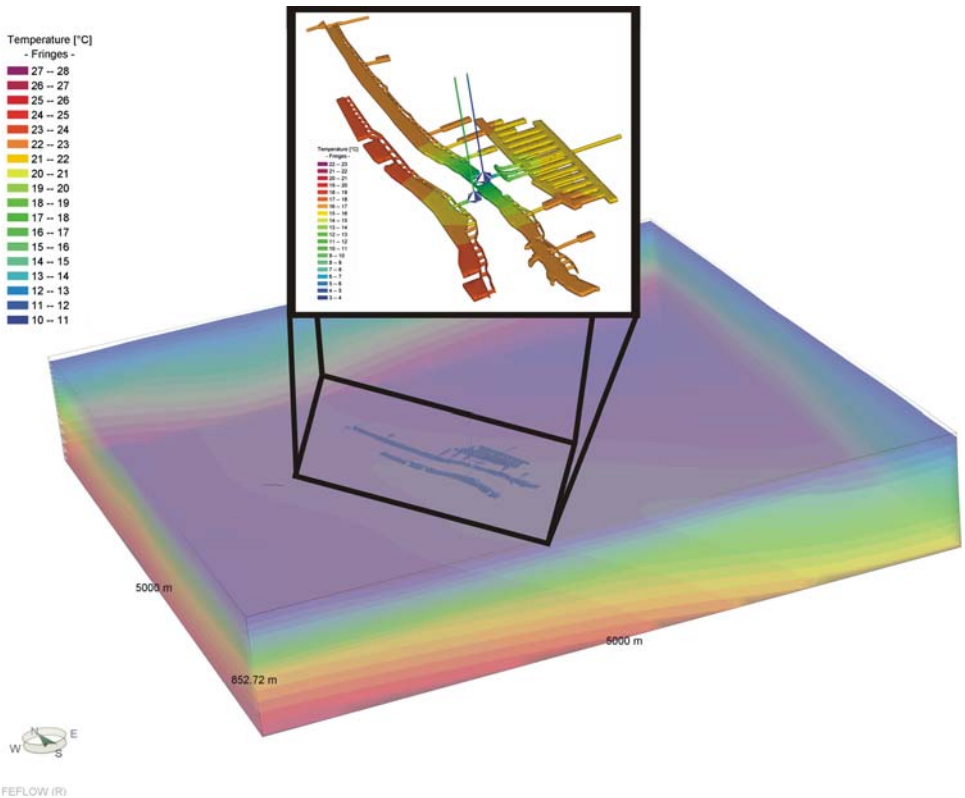

Fig. 14 3-D model showing the calculated temperature, the temperature in the central positioned mine workings is displayed in the enalrged image

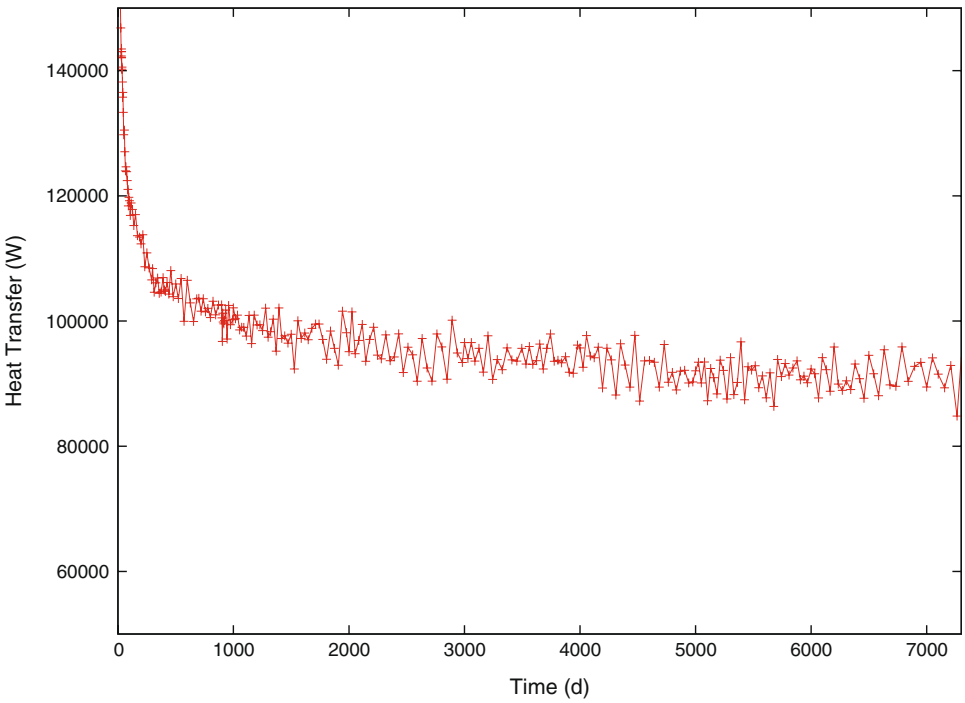

Fig. 15 Temporal heat extracted at the extraction well

In general, more accurate results will be achieved by applying numerical approaches for free water flow in the mine workings, taking the turbulent regime into account. However, for a general survey, calibrated models based on a porous (laminar) approach may be sufficient.

Numerical simulation can be a powerful tool for designing and planning geothermal applications. The computations require the availability of additional parameters such as thermal conductivity and thermal capacity as well as the availability of subsurface temperature measurements.

Besides their use in evaluating a prospective geothermal installation, such data can give substantive and new information on the flow field (see Anderson 2005).

Density differences due to salinity were not considered here as we wanted to focus on temperature effects. A number of articles have already been published on numerical modeling of density changes due to thermohaline flow (e.g., Diersch and Kolditz 2002). Another important subject, geothermal chemical reactions, was also not discussed here; examples can be found, for instance, in Raymond et al. (2008).

Using the open programing interface (IFM) of FEFLOW, future work should include additional approaches to model turbulent flow in mine workings, including testing the well known Darcy–Weisbach approach.

Acknowledgments Some of the data on the geological structure that we used had been collected by fellows within the project "Dynamik abgesoffener oder gefluteter Salzbergwerke und ihres Deckgebirgsstockwerks," which was funded by the Federal Ministry of Education and Research Germany (BMBF) under contract 02 C 1516. However, the presented models should not be considered to accurately represent the subsurface there. We also thank the two anonymous reviewers for their valuable comments.

References

Adams R, Younger PL (2001) A strategy for modeling ground water rebound in abandoned deep mine systems. Ground Water 39:249–261

Adams R, Parkin G (2002) Development of a coupled surface-groundwater-pipe network model for the sustainable management of karstic groundwater. Environ Geol. doi:10.1007/s00254-001-0513-8

Anderson MP (2005) Heat as a ground water tracer. Ground Water 43:951–968

Bazargan Sabet B, Demollin E, Van Bergermeer J-J (2008) Geothermal use of deep flooded mines. In: Proceeding of the Post-Mining, Nancy, pp 1–11

Beardsmore GR, Cull JP (2001) Crustal heat flow. Cambridge University Press, Cambridge, p 324

Brouyère S, Orban P, Wildemeersch S, Couturier J, Gardin N, Dassargues A (2008) The hybrid finite element mixing cell method: a new flexible method for modelling mine water problems. In: Proceedings of the 10th international mine water association congress, Karlovy Vary, pp 429–432

Carslaw HS, Jaeger JC (1959) Conduction of heat in solids. Oxford University Press, London, p 505

Clauser C (2006) Geothermal energy. Landolt-Börnstein, group VIII: advanced materials and technologies. In: Heinloth K (ed) Renewable energies, vol 3(C). Springer, Heidelberg, p 493–604

Clauser C, Heitfeld M, Rosner P, Sahl H, Schetelig K (2005) Nutzung von Erdwärme in aufgelassenen Bergwerken am Beispiel des Aachener Steinkohlenreviers. Beratende Ingenieure 6:14–17

Diersch H-JG (2005) FEFLOW finite element subsurface flow and transport simulation system, reference manual, WASY, Institute for Water Resources Planning and Systems Research, Berlin, 292 pp

Diersch H-JG, Kolditz O (2002) Variable-density flow and transport in porous media: approaches and challenges. Adv Water Resour 25:899–944

Goldberg D (1991) What every computer scientist should know about floating-point arithmetic. ACM Comput Surv 23(1):5–48

Malolepszy Z (2003) Low-temperature, man-made geothermal reservoirs in abandoned workings of underground mines. In: Proceedings of the 28th workshop on geothermal reservoir engineering, Stanford University, USA, pp 259–265

Pruess K (1991) TOUGH2—a general purpose numerical simulator for multiphase fluid and heat flow. Lawrence Berkeley Laboratory report LBL-29400, Berkeley, 102 pp

Rapantova N, Grmela A, Vojtek D, Halir J, Michalek B (2007) Ground water flow modelling applications in mining hydrogeology. Mine Water Environ. doi:10.1007/s10230-007-0017-1

Raymond J, Therrien R (2007) Low-temperature geothermal potential of the flooded Gaspé Mines, Québec, Canada. Geothermics. doi:10.1016/j.geothermics.2007.10.001

Raymond J, Therrien R, Hassani F (2008) Overview of geothermal energy resources in Québec (Canada). In: Proceeding of the 10th international mine water association congress, Karlovy Vary, p 99–100

Trefry MG, Muffels C (2007) FEFLOW: a finite-element ground water flow and transport modeling tool. Ground Water 45(5):525–528

Van Tongeren P, Dreesen R (2004) Residual space volumes in abandoned coal mines of the Belgian Campine basin and possibilities for use. Geologica Belgica 7(3–4):157–164

Watzlaf GR, Ackman TE (2006) Underground mine water for heating and cooling using geothermal heat pump systems. Mine Water Environ. doi:10.1007/s10230-006-0103-9

White W, White E (2005) Ground water flux distribution between matrix, fractures, and conduits: constraints on modeling. Speleogenesis and Evolution of Karst Aquifers 3(2):2–6

Wieber G, Pohl S (2008) Mine water: a source of geothermal energy—examples from the rhenish Massif. In: Proceedings of the 10th international mine water association congress, Karlovy Vary, pp 113–116

Wolkersdorfer C (2008) Water management at abandoned flooded underground mines: fundamentals, tracer tests, modelling, water treatment. Springer, Heidelberg, p 465